Journal of
Ceramic Science
and Technology

J. Ceram. Sci. Tech., **08** [01] 141-148 (2017)
DOI: 10.4416/JCST2016-00103
available online at: http://www.ceramic-science.com
© 2017 Göller Verlag

LSD-based 3D printing of alumina ceramics

A. Zocca*[1], P. Lima[1], J. Günster[1]

[1]BAM Federal Institute for Materials Research and Testing, Division 5.4 Ceramic processing and biomaterials, Unter den Eichen 44 – 46, D-12203 Berlin, Germany

received November 3, 2016; received in revised form December 16, 2016; accepted January 22, 2017

Abstract

An improved method of powder 3D printing leading to dense ceramic parts is presented. The application of powder-based binder jetting 3D printing technologies to technical ceramics is generally limited by the low packing density of the powder and by the need to use a flowable powder. With layer-wise slurry deposition, it is, however, possible to deposit powder beds with high particle packing and furthermore using submicron powders. This method was combined with the binder jetting technology to develop a novel process, named LSD-print. By means of LSD-print, a submicron Al_2O_3 powder could be processed to produce samples with a density comparable with that of standard pressed samples, both in the green state and after sintering.

Keywords: Additive manufacturing, layer-wise slurry deposition, dense alumina, 3D printing

I. Introduction

Additive Manufacturing (AM) is receiving increasing interest from industry and the society, with applications already in the industrial production and in the consumer market.

AM technologies have reached an advanced level of maturity for metallic and polymeric materials, but their maturity for ceramic materials still lags behind significantly. Different AM technologies have been applied to ceramics, each with specific advantages and limitations. A complete overview of AM applied to ceramics can be found in reviews on the topic [1–3]. The current technologies can already produce relatively small and very precise parts with a dense microstructure (in particular, by means of stereolithography [4,5]), scaffolds and log-pile structures with a designed porosity (in particular, with robocasting [6,7]). However, for ceramic materials there is still a need for AM technologies capable of flexibly producing medium to large monolithic parts (wall thickness > 10 – 20 mm), with a high density and properties comparable to parts made with standard processing technologies. For metallic and polymeric materials, powder bed technologies typically fulfill this market. The working principle of powder bed technologies is the successive deposition of thin layers of a powder. In each layer, the cross-section of the part is selectively inscribed, and at the end of the process the part can be cleaned from the surrounding powder bed. One method to inscribe the cross-section is by means of selective laser sintering or melting (SLS/SLM) of the powder. SLS/SLM is widely used for metals, but its application to ceramics is more complex, because the high thermal gradients generated in the process and lack of ductility of these materials make it difficult to achieve parts without defects, even though appreciable densities have been achieved [8]. 3D printing is another powder-based method which consists of ink jetting a binder into the powder layers to selectively bind the particles. At the end of the process, the green part is cleaned from the powder bed and sintered. Powder-based 3D printing is particularly suitable for the production of large parts, because it is easily scalable and the printing heads can consist of up to thousands of jets working in parallel. 3D printers using this technology are already on the market, with printing areas of > 1 m^2. They can also be used for ceramic materials, an important application being, for example, the production of sand casting moulds and cores for metal casting. Their application to high-quality technical ceramics is, however, hindered by the low density of the green parts produced by this process. The formation of layers by deposition of a fine (< 30 µm) dry powder typically achieves a packing density below 50 % T.D. (theoretical density) [9]. Furthermore, only rather coarse particles can be used to obtain a flowable powder, which is necessary for the deposition of the layers. These two factors combined hinder densification during sintering, in some cases making it impossible to achieve dense parts, or necessitating the application of additional post-treatment. In this context, layer-wise slurry deposition (LSD) has been developed for the deposition of powder layers with a high packing density [10–12].

It is based on the spreading of a ceramic slurry by means of a doctor blade, instead of using a dry powder as in the traditional process. Each deposited layer is then dried and treated by a laser (LSD-laser technology, similarly to SLS/SLM) or printed by a printing head (LSD-print technology, similar to 3D printing). The LSD-laser has been successfully applied to silicate ceramics, such as porcelain.

For the application to technical ceramics, a novel LSD-print technology has been recently developed. This

* Corresponding author: andrea.zocca@bam.de

manuscript describes the application of LSD-print to alumina as an example of the potential of this technology for the AM of dense technical ceramics with properties comparable to those obtained in traditional processing.

II. Materials and Methods

The alumina powder used was Almatis CT 3000 SG (Almatis GmbH, Germany), which had a nominal d_{50} = 0.5 µm and a specific surface area of 7.5 m^2/g according to its specifications.

Slurries were produced by ball-milling alumina powder, deionized water and dispersant for 4 h and then adding a sodium alginate (Alginex B-GL, Kimica Corporation, Japan) solution with concentration of 30 g/L until a mass fraction of 0.3 % was reached. The slurry was finally mixed again for 8 h and sieved to remove the milling balls. Any air bubbles left in the slurry were removed by mixing slowly in a roller mill. The resulting slurry had a solids volume fraction of 34 %.

The machine used for the deposition of layers was a custom setup produced by Tools and Technologies GmbH (Schönwald, Germany). The printing setup was developed in collaboration with Voxeljet GmbH (Augsburg, Germany) and uses a piezo SL 128-AA printhead (Fujifilm, Japan).

The printing ink was composed of copper sulfate pentahydrate (Carl Roth GmbH + Co. KG, Germany) dissolved in ethylene glycol (Merck KGaA, Germany) with a concentration of 100 g/L. The drop mass was measured by weighing 30 000 drops for each of the 128 jets and dividing the total weight by the total number of drops. The measurement was repeated five times and averaged.

After printing, the parts were cleaned from the powder bed by washing with deionized water and successively debound at 800 °C and sintered at 1540 °C or at 1600 °C in air. The parts printed for the density measurements had rectangular geometry with dimensions of 25 mm x 10 mm x 1.6 mm.

The density of the green parts was calculated by measuring the mass with a laboratory balance (RC210P, Sartorius, Germany) and the volume by X-ray computer tomography (µCT 42, Scanco Medical AG, Switzerland). The density of the sintered parts was measured with the Archimedes method according to normative ISO 18754 – 2013.

The fracture surface and microstructure of the sintered parts was observed by means of a scanning electron microscope (ZEISS Gemini Supra 40, Carl Zeiss AG, Oberkochen, Germany).

III. Results and Discussion

(1) LSD-print

The LSD deposition setup and method has been extensively presented in previous publications [10–13]. A schematic of the setup used is shown in Fig. 1. Briefly, a layer of ceramic slurry is deposited on a base substrate by means of a doctor blade and dried. After the first layer, another slurry layer is deposited on top and dried. It is important to notice that the substrate for the deposition of the second and the successive layers is formed by the previous powder layers, which act as a porous mold. Already during the deposition, water is drawn from the slurry into the pores of the previous layers by capillary forces, and a cast grows in a similar way as in the slip casting process. This mechanism is responsible for the high powder packing density achievable with LSD, which depending on the material system used is in the range of 55 – 70 % T.D.

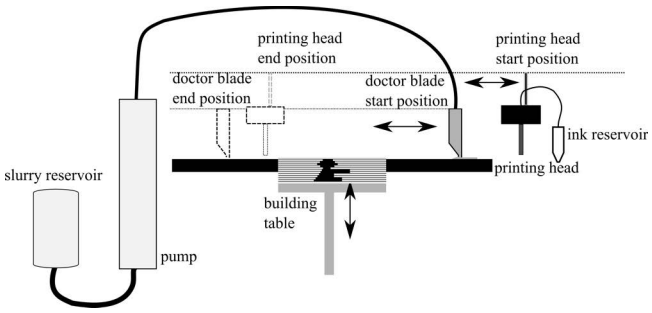

Fig. 1: Schematic of the layer-wise slurry deposition setup in combination with binder jetting 3D printing (LSD-print).

In the LSD-print process, the cross-section of the part is printed in each layer using an ink-jetting technology.

There are several combinations of ink compositions and additives in the slurry which can be used to locally and selectively bind the particles. At the end of the process, the part is embedded in a block of highly packed powder particles and it needs to be released from it by washing in water. For this reason, an important requisite of the "slurry + ink" system used is that the powder layers should be redispersible in water, and the printed part should become not only stronger than the surrounding powder, but also non-dispersible in water.

(2) Alginate binder system for Al_2O_3 slurries

A possible binding mechanism, which has been investigated in this study, is the cross-linking of sodium alginate by bivalent cations.

Sodium alginate is the salt of alginic acid, a natural anionic polysaccharide. It is extracted from brown algae and is non-toxic, even used as a food additive. This makes it environmentally friendly compared to the typical additives, such as cross-linkable monomers, used in other additive manufacturing processes. Sodium alginate is a linear copolymer composed of blocks of β-D mannuronate (M) and α-L-guluronate (G) residues. It is known that sodium alginate can be cross-linked with the addition of multivalent (particularly bivalent) cations. G blocks bind the cations stronger than M blocks, therefore alginates rich in G produce strong and brittle gels, while alginates rich in M form soft and deformable gels [14]. For this reason, a type of alginate with high G content was chosen for this process (Alginex B-GL by Kimica Corporation, Japan). It is also known that different cations have a different affinity to the alginate and also a different concentration needed to cross-link it. Haug *et al.* showed that the concentration of ions necessary to induce gel formation follows this order: $Ba^{2+} < Pb^{2+} < Cu^{2+} < Sr^{2+} < Cd^{2+} < Ca^{2+} < Zn^{2+} < Ni^{2+} < Co^{2+} < Mn^{2+}$, $Fe^{2+} < Mg^{2+}$ [15]. As it is difficult to for-

mulate printable inks with Ba salts and given the toxicity of Pb, Cu^{2+} was selected as cation for the cross-linking of the alginate.

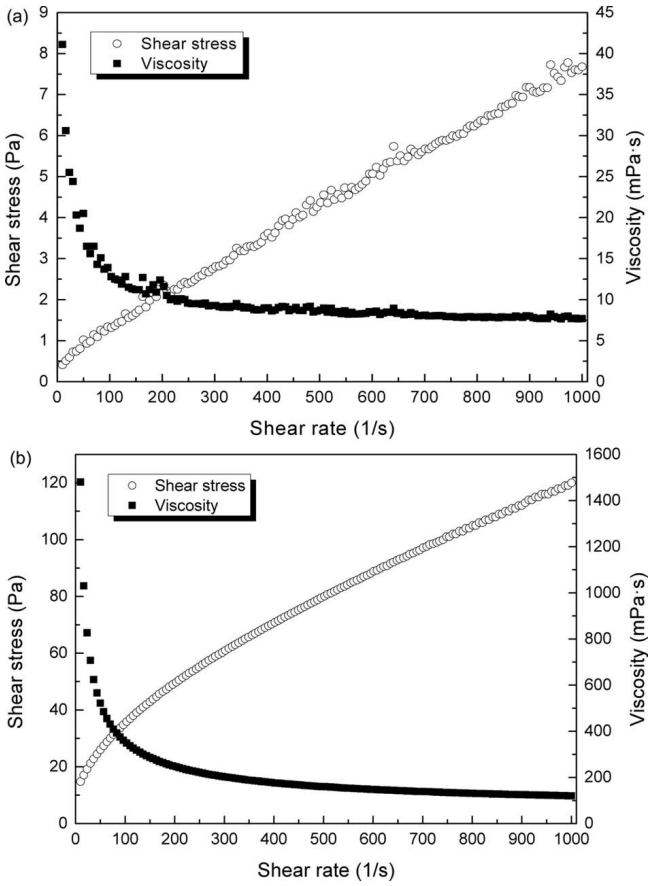

Fig. 2: Flow and viscosity curves for the alumina slurry without (a) and with (b) alginate.

The gelation of alginate has already been used in the gel-casting process to produce complex ceramic parts [16–19]. In the gel casting process, typically a slurry is produced which already contains alginate and the source of bivalent ions (typically Ca^{2+}), together with a chelator which prevents the ions cross-linking the alginate. The slurry is then poured into a mold and an activator is added to release the ions and gel the part.

In the LSD-print, the bivalent ions are added in the ink and selectively printed in the layers. It is important to note that the layers are dried before printing. The printed ink provides therefore not only the bivalent cations, but also the liquid environment necessary for the transport of the ions and for their reaction with alginate. At the end of the process, the entire powder bed is washed in water and the printed part remains jelly, while the surrounding powder can be dispersed. In comparison to the alginate gel-casting system, there is no need to add the chelator and the activator to the slurry, since the ions are printed selectively only into the part.

The alginate has a secondary role, which is to improve the rheological properties of the slurry for the deposition process and to act as a binder in the green layers, preventing cracking during drying.

Indeed, alginate has been used as reported in the literature as an additive for tape casting [20–22].

Fig. 2 shows the rheological flow curve for the alumina slurry used in the current study, before (a) and after (b) the addition of the alginate, that is 0.3 wt% of the slurry.

It can be noticed that the addition of the alginate increased the viscosity of the slurry and caused a higher shear-thinning behavior. Both these factors were favorable because they contributed to achieving a more homogeneous flow of the slurry during deposition.

(3) Characterization of LSD-printed parts

Fig. 3 and Fig. 4 show the sequence of post-treatments of two alumina toothed wheels produced by means of LSD-print. The parts were initially embedded in the powder bed (Fig. 3a) and were released by careful rinsing with deionized water (Fig. 3b). The resulting green bodies (Fig. 4a) were successively debound to remove the alginate and finally sintered (Fig. 4b).

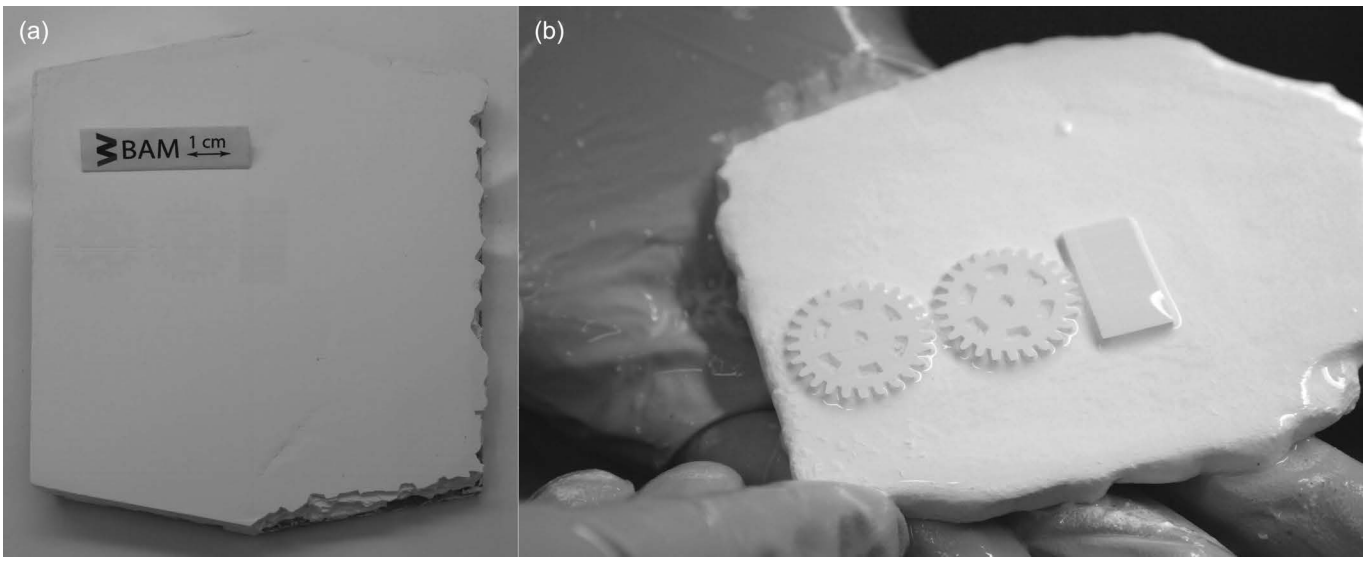

Fig. 3: Alumina LSD-printed toothed wheels (a) embedded in the powder bed at the end of the process and (b) after partial removal by washing with water.

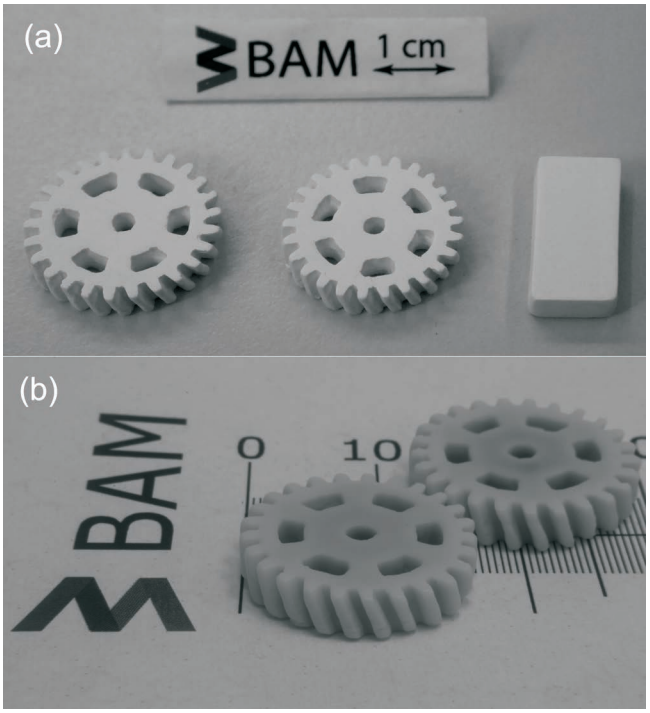

Fig. 4: LSD-printed Al_2O_3 toothed wheels – green bodies (a) and sintered (b).

It should be noted that the amount of alginate used was very small (0.3 wt% of the slurry), therefore debinding was straightforward. Other additive manufacturing technologies for ceramics, such as stereolithography, make use of up to 60 vol% organics, and for this reason debinding is typically complex and limited to a maximum wall thickness.

The cross-linking of the alginate with divalent cations could be used as binding mechanism to produce complex parts. Despite the good definition and surface quality of the parts after washing, the jelly state of the parts limited the minimum size of printed features.

Table 1 reports some properties of LSD-printed parts sintered at 1540 °C and 1600 °C.

It is remarkable that a density of 3.91 g/cm^3 at 1540 °C and of 3.94 g/cm^3 at 1600 °C corresponds to the density values declared in the data sheet of the Al_2O_3 powder used (CT3000 SG, Almatis GmbH, Germany) for samples uniaxially pressed at 90 MPa resulting in a green density of 2.25 g/cm^3. The green density is similar to the density of the as-printed green body determined by µCT, which was approx. 2.27 g/cm^3. For comparison, few applications of powder-bed technologies to technical ceramics, such as Al_2O_3, are described in the literature. Some early work by Cima *et al.* reported on the 3D printing (binder jetting) of agglomerates of a submicron Al_2O_3 powder [23]. The as-printed green parts had a density 31 – 34 % T.D., which, as expected, led to a sintered density at 1650 °C of only 62.5 % T.D. The application of warm isostatic pressing to the parts and the addition of MgO as dopant could increase the sintered density to 99.2 % T.D., but restricts the geometry. Subramanian *et al.* processed an Al_2O_3 powder with an average particle size of 2 µm by agglomerating it to 100 µm size and spray coating it with a polymeric binder. This powder was used for the selective laser sintering process, producing green parts with a density of ca. 40 – 45 % T.D. These parts could be sintered to a density < 2.3 g/cm^3 at 1600 °C, which is ca. 58 % T.D. [24].

Another possible post-treatment is the infiltration of the parts after sintering. Melcher *et al.* 3D-printed the same Al_2O_3 powder used in the current study (Almatis CT3000 SG). The printed green parts had a minimum porosity of 52 % and of 33 % after sintering at 1600 °C, showing that it was not possible to sinter the parts to full density. A post-infiltration of the samples with a mixture of Cu and CuO was employed to obtain dense Al_2O_3/Cu-O composites [25].

In Table 1, it is also noteworthy that the sintering shrinkage was anisotropic. It is common in powder bed processes to have a different shrinkage in Z (perpendicular to the layers) compared to X-Y (parallel to the layers) [26]. The small difference of approximately 1 % between X (in the plane of the layers and parallel to the movement of the doctor blade) and Y (in the plane of the layers and perpendicular to the movement of the doctor blade) might be related to some degree of alignment of the alginate polymeric chains parallel to the deposition direction. The shrinkage in the three directions was anyways reproducible and it could be compensated in the design of the component.

The drop mass measured was ca. 83 ng, which corresponded to a concentration of 0.072 mol Cu^{++} for each gram of alginate. For comparison, in the gel-casting of ceramic suspensions with alginate, a concentration of Ca^{++} in the range of 0.0013 – 0.017 mol Ca^{++} for each gram of alginate has been used [16 – 19, 21, 27 – 30].

From the measured drop mass, it could also be estimated that the concentration of $CuSO_4{\cdot}5H_2O$in the printed parts was approx. 0.82 wt%, which could possibly amount to a CuO concentration in the final part of about 0.26 wt%. CuO in this concentration range can act as a sintering aid and, thus, improve the sintering of the alumina body, even though it should be taken into account that it has a slight effect on promoting grain growth [31, 32].

Table 1: Properties of Al_2O_3 LSD-printed green samples and after sintering at 1540 °C or 1600 °C. Z= direction perpendicular to the layers; X= in plane of the layers and parallel to the movement of the doctor blade; Y= in plane of the layers and perpendicular to the movement of the doctor blade.

	Density (g/cm^3)	Shrinkage X (%)	Shrinkage Y (%)	Shrinkage Z (%)	Mass Loss (%)
Sintered at 1540 °C	3.91 ± 0.01	14.7 ± 0.1	15.7 ± 0.1	18.5 ± 0.1	1.77 ± 0.02
Sintered at 1600 °C	3.94 ± 0.01	14.9 ± 0.1	16.1 ± 0.1	19.2 ± 0.1	1.81 ± 0.01

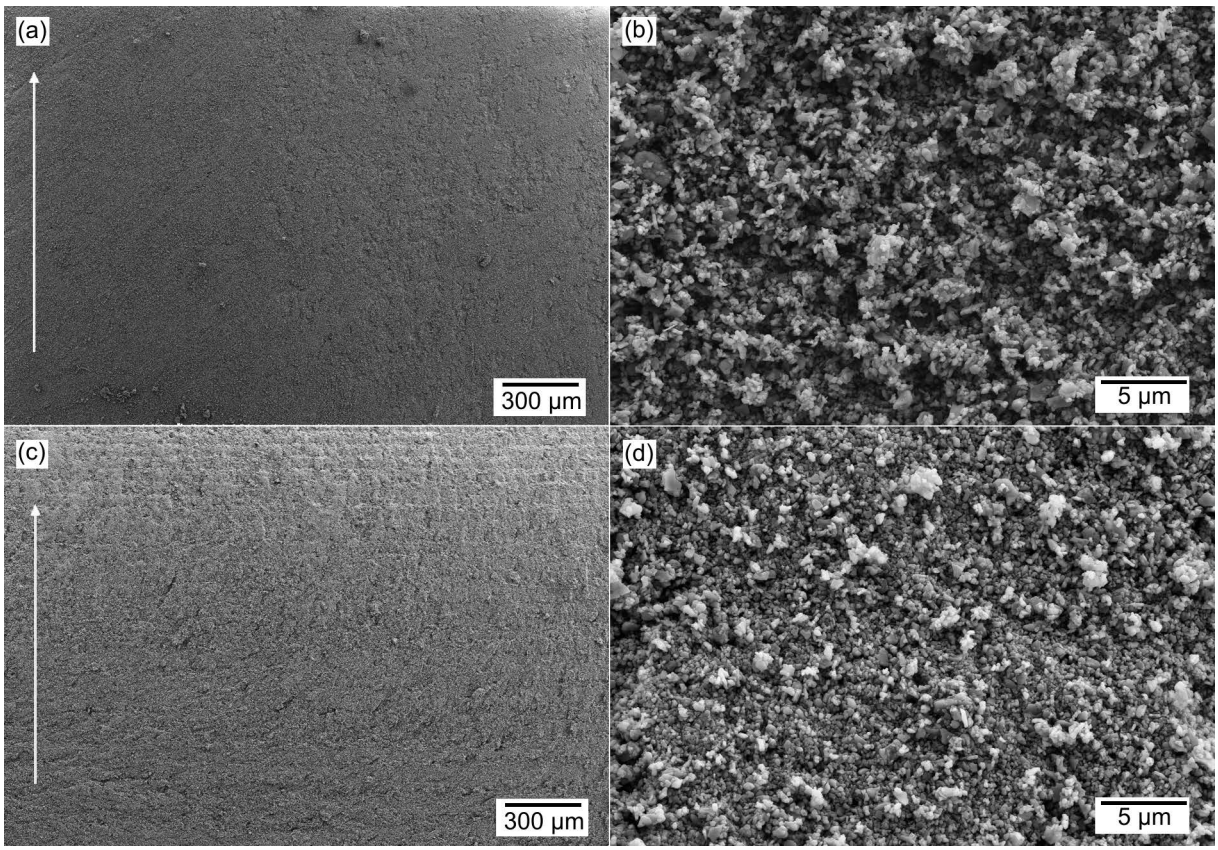

Fig. 5: SEM micrographs of the fracture surface of the cross-section of Al_2O_3 green layers deposited by LSD with a layer thickness of 50 µm (a,b) and of the corresponding green LSD-printed part (c,d). The arrows indicate the buildup direction.

Fig. 5 shows SEM images of the cross-section of green layers deposited by the LSD of the alumina slurry. Fig. 5 confirmed the good packing of the ceramic particles, in agreement with the relatively high green density of the LSD-printed parts.

The interphase between layers was not visible in most of the fracture surfaces examined, as showed in Fig. 5a. This highlights the good joining between layers in the LSD process, which is related to the slip casting phenomenon during deposition of the ceramic slurry.

Figs. 5c, d show the fracture surface of the cross-section of an LSD-printed green part. In Fig. 5c, the layers are barely visible, but no clear interface was observed at higher magnification. Small gradients in the composition of the layers might be responsible for this effect, because smaller particles and the alginate binder may tend to migrate to the bottom of the layer in the slip casting process during deposition.

Fig. 6 shows the cross-section of the fracture surface of an LSD-printed part sintered at 1540 °C. The SEM analysis confirmed the absence of macroscopic defects and the high density achieved, in agreement with the results listed in Table 1. The fracture surface after sintering also did not show any layer interface or preferential path for the fracture, which indicates a complete joining of the layers during sintering.

The top view of samples sintered at 1540 °C (Fig. 7a) and 1600 °C (Fig. 7b) also revealed a fine-grained and homogeneous microstructure, with, as expected, a slightly higher density and grain growth at the higher temperature.

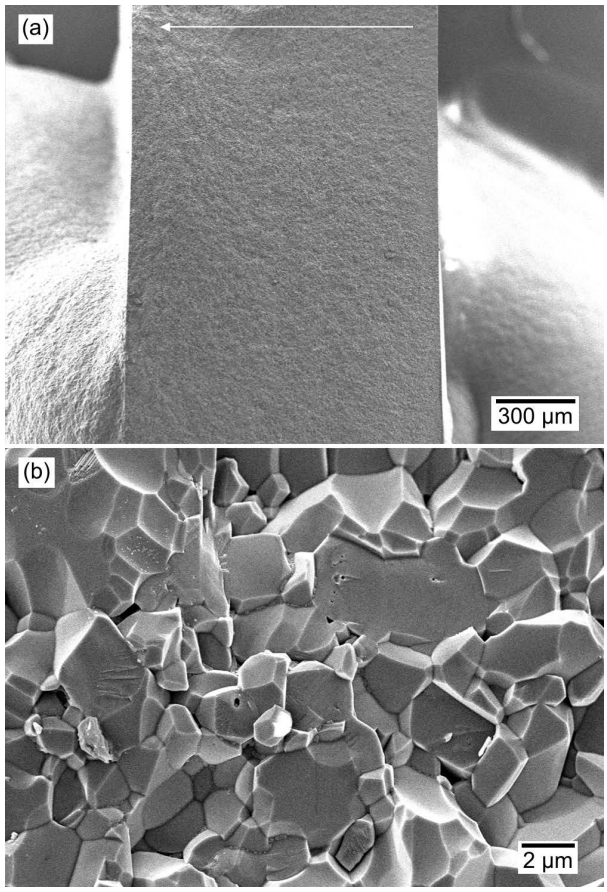

Fig. 6: SEM micrographs of the fracture surface of the cross-section of an Al_2O_3 LSD-printed part sintered at 1540 °C. The arrow indicates the buildup direction.

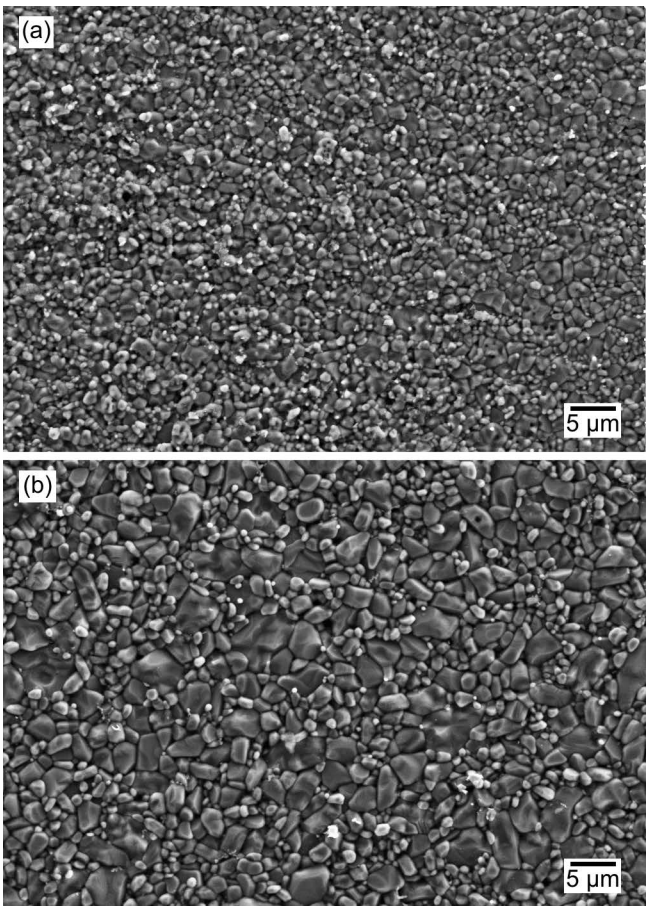

Fig. 7: SEM micrographs of the top view of Al_2O_3 LSD-printed samples sintered at 1540 °C (a) and 1600 °C (b).

IV. Conclusions

Layer-wise slurry deposition 3D printing (LSD-print) was demonstrated for the first time and it was applied to a fine Al_2O_3 ceramic powder. Complex-shaped alumina parts with good definition could be printed, which had a high green density and a high density after sintering, comparable to reference parts produced by means of standard shaping technologies, such as uniaxial pressing.

The low amount of binder used (0.3 wt% of the slurry) allows the additive manufacturing of large components by LSD-print, which combined with the high density achieved is a unique characteristic of LSD-print, compared to the other additive manufacturing technologies applied to ceramics.

The cross-linking of alginate with divalent cations could be used to produce complex LSD-printed parts. Different binder systems will be investigated in the future, in order to obtain parts that are easier to clean and with even thinner features.

References

1 Zocca, A., Colombo, P., Gomes, C.M., Günster, J.: Additive manufacturing of Ceramics: Issues, potentialities, and opportunities, *J. Am. Ceram. Soc.,* **98**, 1983 – 2001, (2015).

2 Travitzky, N., Bonet, A., Dermeik, B., Fey, T., Filbert-Demut, I., Schlier, L., Schlordt, T., Greil, P.: Additive manufacturing of ceramic-based materials, *Adv. Eng. Mater.,* **16**, 729 – 754, (2014).

3 Deckers, J., Vleugels, J., Kruth, J.-P.: Additive manufacturing of ceramics: A review, *J. Ceram. Sci. Tech.,* **5**, 245 – 260, (2014).

4 Kirihara, S.: Creation of functional ceramics structures by using stereolitographic 3D printing, *Trans. JWRI,* **43**, 5 – 10, (2014).

5 Schwentenwein, M., Homa, J.: Additive manufacturing of dense alumina ceramics. *Int. J. Appl. Ceram. Technol.,* **12**, 1 – 7, (2015).

6 Zocca, A., Franchin, G., Elsayed, H., Gioffredi, E., Bernardo, E., Colombo, P.: Direct ink writing of a preceramic polymer and fillers to produce hardystonite ($Ca_2ZnSi_2O_7$) bioceramic scaffolds, *J. Am. Ceram. Soc.,* **99**, 1960 – 1967, (2016).

7 Smay, J.E., Cesarano, J., Lewis, J.A.: Colloidal inks for directed assembly of 3-D periodic structures, *Langmuir,* **18**, 5429 – 5437, (2002).

8 Juste, E., Petit, F., Lardot, V., Cambier, F.: Shaping of ceramic parts by selective laser melting of powder bed, *J. Mater. Res.,* **29**, 2086 – 2094, (2014).

9 Zocca, A., Gomes, C.M., Mühler, T., Günster, J.: Powder-bed stabilization for powder-based additive manufacturing, *Adv. Mech. Eng.,* **6**, 491581, (2014).

10 Mühler, T., Gomes, C.M., Heinrich, J., Günster, J.: Slurry-based additive manufacturing of ceramics, *Int. J. Appl. Ceram. Technol.,* **12**, 18 – 25, (2015).

11 Tian, X., Günster, J., Melcher, J., Li, D., Heinrich, J.G.: Process parameters analysis of direct laser sintering and post treatment of porcelain components using Taguchi's method, *J. Eur. Ceram. Soc.,* **29**, 1903 – 1915, (2009).

12 Gahler, A., Heinrich, J.G., Guenster, J.: Direct laser sintering of Al_2O_3-SiO_2 dental ceramic components by layer-wise slurry deposition, *J. Am. Ceram. Soc.,* **89**, 3076 – 3080, (2006).

13 Tian, X., Li, D., Heinrich, J.G.: Rapid prototyping of porcelain products by layer-wise slurry deposition (LSD) and direct laser sintering, *Rapid Prototyp. J.,* **18**, 362 – 373, (2012).

14 Gacesa, P.: Alginates, *Carbohydr. Polym.,* **8**, 161 – 182, (1988).

15 Haug, A., Smidsrød, O.: The effect of divalent metals on the properties of alginate solutions, *Acta Chem. Scand.,* **19**, 341 – 351, (1965).

16 Akhondi, H., Taheri-Nassaj, E., Sarpoolaky, H., Taavoni-Gilan, A.: Gelcasting of alumina nanopowders based on gelation of sodium alginate, *Ceram. Int.,* **35**, 1033 – 1037, (2009).

17 Jia, Y., Kanno, Y., Xie, Z.: New gel-casting process for alumina ceramics based on gelation of alginate. *J. Eur. Ceram. Soc.*, **22**, 1911 – 1916, (2002).

18 Jia, Y., Kanno, Y., Xie, Z.-P.: Fabrication of alumina green body through gelcasting process using alginate. *Mater. Lett.,* **57**, 2530 – 2534, (2003).

19 Wang, X., Xie, Z.-P., Huang, Y., Cheng, Y.-B.: Gelcasting of silicon carbide based on gelation of sodium alginate, *Ceram. Int.,* **28**, 865 – 871, (2002).

20 Santacruz, I., Gutiérrez, C.A., Nieto, M.I., Moreno, R.: Application of alginate gelation to aqueous tape casting technology, *Mater. Res. Bull.,* **37**, 671 – 682, (2002).

21 Yu, Z., Huang, Y., Wang, C., Ouyang, S.: A novel gel tape casting process based on gelation of sodium alginate, *Ceram. Int.,* **30**, 503 – 507, (2004).

22 Carisey, T., Laugier-Werth, A., Brandon, D.G.: Control of texture in Al_2O_3 by gel-casting, *J. Eur. Ceram. Soc.,* **15**, 1 – 8, (1995).

23 Cima, M.J., Yoo, J., Khanuja, S., Rynerson, M., Nammour, D., Giritlioglu, B., Grau, J., Sachs, E.M.: Structural ceramic components by 3d printing. In: Proceedings of the Solid Freeform Fabrication Symposium. University of Texas, Austin, Texas, 1995.

24 Subramanian, K., Vail, N., Barlow, J., Marcus, H.: Selective laser sintering of alumina with polymer binders, *Rapid Prototyp. J.,* **1**, 24 – 35, (1995).

[25] Melcher, R., Martins, S., Travitzky, N., Greil, P.: Fabrication of Al_2O_3-based composites by indirect 3D-printing, *Mater. Lett.,* **60**, 572 – 575, (2006).

[26] Gaytan, S.M., Cadena, M.A., Karim, H., Delfin, D., Lin, Y., Espalin, D., MacDonald, E., Wicker, R.B.: Fabrication of barium titanate by binder jetting additive manufacturing technology, *Ceram. Int.,* **41**, 6610 – 6619, (2015).

[27] Akhondi, H., Taheri-Nassaj, E., Taavoni-Gilan, A.: Gelcasting of alumina-zirconia-yttria nanocomposites with Na-alginate system, *J. Alloy. Compd.,* **484**, 452 – 457, (2009).

[28] Ma, J., Xie, Z., Miao, H., Zhang, B., Lin, X., Cheng, Y.: Gelcasting of alumina ceramic components in nontoxic Na-alginate-$CaIO_3$-PVP systems, *Mater. Des.,* **26**, 291 – 296, (2005).

[29] Xie, Z., Huang, Y., Chen, Y., Jia, Y.: A new gel casting of ceramics by reaction of sodium alginate and calcium iodate at increased temperatures, *J. Mater. Sci. Lett.,* **20**, 1255 – 1257, (2001).

[30] Xie, Z., Wang, X., Jia, Y., Huang, Y.: Ceramic forming based on gelation principle and process of sodium alginate, *Mater. Lett.,* **57**, 1635 – 1641, (2003).

[31] Cahoon, H.P., Christensen, C.J.: Sintering and grain growth of alpha-alumina, *J. Am. Ceram. Soc.,* **39**, 337 – 344, (1956).

[32] Ramesh, S., Aw, K.L., Ting, C.H., Tan, C.Y., Sopyan, I., Teng, W.D.: Effect of copper oxide on the sintering of alumina ceramics, *Adv. Mater. Res.,* **47 – 50**, 801 – 804, (2008).